# Determining attenuation properties of interfering fast and slow ultrasonic waves in cancellous bone

Amber M. Nelson, Joseph J. Hoffman, Christian C. Anderson,[a] and Mark R. Holland
*Department of Physics, Washington University in Saint Louis, Saint Louis, Missouri 63130*

Yoshiki Nagatani
*Department of Electronics, Kobe City College of Technology, Kobe 651-2194, Japan*

Katsunori Mizuno and Mami Matsukawa
*Laboratory of Ultrasonic Electronics, Doshisha University, Kyotanabe, Kyoto 610-0321, Japan*

James G. Miller[b]
*Department of Physics, Washington University in Saint Louis, Saint Louis, Missouri 63130*

(Received 6 June 2011; revised 26 July 2011; accepted 26 July 2011)

Previous studies have shown that interference between fast waves and slow waves can lead to observed negative dispersion in cancellous bone. In this study, the effects of overlapping fast and slow waves on measurements of the apparent attenuation as a function of propagation distance are investigated along with methods of analysis used to determine the attenuation properties. Two methods are applied to simulated data that were generated based on experimentally acquired signals taken from a bovine specimen. The first method uses a time-domain approach that was dictated by constraints imposed by the partial overlap of fast and slow waves. The second method uses a frequency-domain log-spectral subtraction technique on the separated fast and slow waves. Applying the time-domain analysis to the broadband data yields apparent attenuation behavior that is larger in the early stages of propagation and decreases as the wave travels deeper. In contrast, performing frequency-domain analysis on the separated fast waves and slow waves results in attenuation coefficients that are independent of propagation distance. Results suggest that features arising from the analysis of overlapping two-mode data may represent an alternate explanation for the previously reported apparent dependence on propagation distance of the attenuation coefficient of cancellous bone. © *2011 Acoustical Society of America*. [DOI: 10.1121/1.3625241]

PACS number(s): 43.80.Ev, 43.80.Qf, 43.20.Hq, 43.20.Ye [CCC] Pages: 2233–2240

## I. INTRODUCTION

Although dual-energy x-ray absorptiometry (DXA) is the current gold standard for diagnosing osteoporosis, quantitative ultrasound represents an approach for evaluating the quality of cancellous bone that has the potential for determining the likelihood of osteoporosis.[1–3] In Japan, ultrasonic screening for osteoporosis is recommended by the government and is included in the public annual health check. Cancellous bone is a porous material consisting of a matrix of solid trabeculae filled with soft bone marrow. The heterogenous structure of cancellous bone can result in the propagation of complicated ultrasonic waveforms that obfuscate measurements and make the interpretation of results difficult.

Cancellous bone is known to support the propagation of two compressional wave modes, often referred to as fast waves and slow waves.[4–10] In some experimental situations, the two waves are separated in the time-domain data, whereas in other circumstances the two waves substantially overlap and may appear as only a single wave. The degree to which the fast waves and slow waves overlap depends on a number of factors including porosity, structural anisotropy, ultrasonic path length, and the angle of insonification relative to the predominant trabecular orientation.[5,8,11,12]

When the fast waves and slow waves are clearly distinct and separated in time in the radio frequency data, each mode can be analyzed individually to obtain intrinsic ultrasonic properties such as the attenuation coefficient and phase velocity. However, under circumstances in which there is overlap between the two wave modes, conventional analysis methods may suggest potentially misleading material properties. Previous studies have demonstrated that interfering fast wave and slow wave modes can account for the apparent negative dispersion sometimes observed in measurements of cancellous bone.[13–17] This apparent negative dispersion arises when conventional phase spectroscopy analysis of two overlapping waves is performed as if only one wave were present. Sometimes the presence of an additional wave is not apparent in the RF signal.

One objective of the current study was to examine the effects of interfering fast and slow waves on the determination of the attenuation properties of cancellous bone. A second objective was to investigate the influence of the choice of methods employed to extract the attenuation properties.

[a]Current address: MIT Lincoln Laboratory, 244 Wood Street, Lexington, MA 02420.
[b]Author to whom correspondence should be addressed. Electronic mail: james.g.miller@wustl.edu

## II. METHODS

In this study, two methods for determining the attenuation properties as a function of propagation distance were applied to the same simulated data to permit a comparison of the relative advantages and disadvantages of the two methods of analysis. The two methods of analysis include a previously reported time-domain technique[18] and a frequency-domain technique performed on separated fast and slow waves. Details of these methods of analysis are presented later in this section.

### A. Generating simulated ultrasonic waves

The experimental observations that provided the basis for the simulated data employed in this study were reported in a manuscript by Nagatani *et al.*[18] In that study, through-transmission measurements were conducted on a $20 \times 20 \times 15$ mm sample from a bovine femoral head, which was immersed in degassed water. Planar PVDF transmitting and receiving transducers were separated by 60 mm. The transmitter was excited by a single cycle of a 1 MHz sinusoid. The direction of wave propagation was parallel to the predominant bone axis. To investigate whether the fast wave attenuation properties were influenced by the thickness of the sample and thus the propagation distance, in that earlier study the specimen was gradually shortened from 15 mm to 6 mm in steps of 1 mm by removing bone tissue from one end of the sample.

In the present work, signals presented in that previous study were employed in conjunction with a model that explicitly accounts for the presence of fast and slow wave modes.[15,19] The ultrasonic propagation through bone was modeled as

$$\text{Output}(f) = \text{Input}(f)[H_{\text{fast}}(f) + H_{\text{slow}}(f)], \tag{1}$$

where Output($f$) and Input($f$) are the complex Fourier spectra of the received mixed mode waveform and the incident waveform, respectively, and $H_{\text{fast}}(f)$ and $H_{\text{slow}}(f)$ are the transfer functions for the fast and slow waves. In this study, the input wave was taken as the reference water-path only signal from the Nagatani *et al.* paper, which is shown in panel (a) of Fig. 7 of that paper.[18] The transfer functions for the individual fast and slow waves are given by

$$H_{\text{fast}}(f) = A_{\text{fast}} \exp(-\beta_{\text{fast}} f d) \exp\left(\frac{i2\pi f d}{c_{\text{fast}}(f)}\right), \tag{2}$$

$$H_{\text{slow}}(f) = A_{\text{slow}} \exp(-\beta_{\text{slow}} f d) \exp\left(\frac{i2\pi f d}{c_{\text{slow}}(f)}\right), \tag{3}$$

in which $A_{\text{fast}}$ and $A_{\text{slow}}$ are frequency-independent signal loss parameters, $\beta_{\text{fast}}$ and $\beta_{\text{slow}}$ are the slopes of attenuation for the fast and slow waves, $d$ is the sample thickness, and $c_{\text{fast}}(f)$ and $c_{\text{slow}}(f)$ are the phase velocities for the fast and slow waves. The phase velocities of the fast and slow waves were required to satisfy the Kramer-Kronig relations for media exhibiting linear-with-frequency attenuation coefficients,[20–25] thus having the following form

$$c_{\text{fast}}(f) = c_{\text{fast}}(f_0) + [c_{\text{fast}}(f_0)]^2 \frac{\beta_{\text{fast}}}{\pi^2} \ln\left(\frac{f}{f_0}\right), \tag{4}$$

$$c_{\text{slow}}(f) = c_{\text{slow}}(f_0) + [c_{\text{slow}}(f_0)]^2 \frac{\beta_{\text{slow}}}{\pi^2} \ln\left(\frac{f}{f_0}\right), \tag{5}$$

where $f_0$ is a reference frequency taken from within the experimental bandwidth, usually at or near midband. In our calculations, $f_0$ was set at 1 MHz, which was the frequency of the excitation pulse.

The parameters in Eqs. (1)–(5) [$A_{\text{fast}}$, $A_{\text{slow}}$, $\beta_{\text{fast}}$, $\beta_{\text{slow}}$, $c_{\text{fast}}(f_0)$, $c_{\text{slow}}(f_0)$] were estimated using Bayesian probability theory applied to the reference water-only signal and the sample signal traveling through 9 mm of bone from the Nagatani *et al.* paper [panels (a) and (b) from Fig. 7, respectively].[18] More detailed explanations of Bayesian parameter estimation can be found in Anderson *et al.*,[19] Bretthorst *et al.*,[26] and Marutyan *et al.*[27] The values of the six parameters used in the propagation model above are given in Table I. Once these six parameters were known, the individual fast and slow waves could be generated for each sample thickness $d$, which was varied from 6 to 15 mm in 1 mm increments.

### B. Methods of analysis of attenuation properties

The two analysis methods discussed in this section were applied to the simulated data generated using the propagation model above.

#### 1. Time-domain analysis of unseparated wave

The method of analysis used in this section is described in the Nagatani *et al.* paper.[18] Its use was suggested by the limitations imposed by the overlapping wave modes. In this time-domain technique, the amplitudes of the first peak of the received signal, which are assumed to correspond to the fast waves, are compared for a series of sample thicknesses. The apparent attenuation value, $\alpha_{\text{time}}$, of the fast wave is defined by

$$\alpha_{\text{time}} = \frac{20 \log(V_n / V_{n+1})}{\Delta d}, \tag{6}$$

where $V_n$ and $V_{n+1}$ are the amplitudes of the first arriving peaks in the received RF waveforms. The indices $n$ and $n+1$ correspond to successive sample thicknesses differing by $\Delta d = 1$ mm.

TABLE I. The values used for the six parameters in the propagation model. This set of parameter values was used because it maximized the posterior probability of the model.

| | $A_{\text{fast}}$ | $A_{\text{slow}}$ | $\beta_{\text{fast}}$ (dB/cm/MHz) | $\beta_{\text{slow}}$ (dB/cm/MHz) | $c_{\text{fast}}$ at 1 MHz (m/s) | $c_{\text{slow}}$ at 1 MHz (m/s) |
|---|---|---|---|---|---|---|
| Bayesian estimate | 1.00 | 0.13 | 49.2 | 7.1 | 1933 | 1475 |

This analysis method was employed to determine the apparent attenuation of the fast waves, but not the slow waves. This choice was made because the amplitudes of the slow waves were sometimes affected by interference from the fast waves, thus leading to meaningless determination of the attenuation of the slow waves.[18]

#### 2. Frequency-domain analysis of separated fast waves and slow waves

The frequency-domain method of determining the attenuation coefficient of a sample (dB/cm) is carried out by performing a log-spectral subtraction technique,[28]

$$\alpha(f) = \frac{10\log\left(\left|\tilde{V}_n(f)\right|^2\right) - 10\log\left(\left|\tilde{V}_{n+1}(f)\right|^2\right)}{\Delta d}, \qquad (7)$$

where $\left|\tilde{V}_n(f)\right|$ and $\left|\tilde{V}_{n+1}(f)\right|$ are the magnitudes of the Fourier transforms of the received signals when the sample has a thickness corresponding to length indices $n$ and $n+1$, respectively, and $\Delta d = 1$ mm. Typically, a through-sample power spectrum is subtracted from a water-only reference power spectrum. In the present study, to apply this frequency-domain analysis method in a fashion analogous to that used in the time-domain analysis method described above, differences between spectra at thickness indices $n$ and $n+1$ were analyzed. Determining the attenuation coefficient using the difference of two through-sample power spectra eliminated the need for compensating for the insertion losses at the boundaries.

In this method, Eq. (7) was applied to the isolated fast wave signal and the isolated slow wave signal. This method of analysis is expected to yield the attenuation coefficient of only the fast wave, free from artifacts caused by interference with the slow wave, and visa versa. The attenuation coefficients corresponding to the fast wave and the slow wave will be referred to as $\alpha_{\text{fast}}$ (f) and $\alpha_{\text{slow}}$ (f), respectively.

## III. RESULTS

### A. Simulated ultrasonic waves

Simulated ultrasonic data were generated using the model in Eqs. (1)–(5) for sample thicknesses ranging in 1 mm steps from 6 mm to 15 mm. Examples of the simulated sample waveforms along with the input reference waveform from the Nagatani *et al.* paper[18] are shown in Fig. 1. Fast and slow waves can be observed in all of the sample traces. As the sample thickness and thus propagation distance were increased, the fast wave was highly attenuated relative to the slow wave.

### B. Time-domain analysis results of unseparated wave

The attenuation value $\alpha_{\text{time}}$ of the fast wave at specific propagation distances within the sample was determined from the peak amplitudes of fast waves that had traversed different sample thicknesses 6, 7, 8,…,15 mm. Figure 2 shows the attenuation $\alpha_{\text{time}}$ of the fast wave as a function of propagation distance. Similar to the results reported in the Nagatani *et al.* paper, the results depicted in Fig. 2 show that the attenuation of the fast wave appears to be larger at the beginning of propagation and then gradually smaller as the wave travels farther into the sample.[18]

### C. Frequency-domain analysis results of separated fast waves and slow waves

The propagation model and Bayesian probability theory analysis used in this study permitted the separation of the

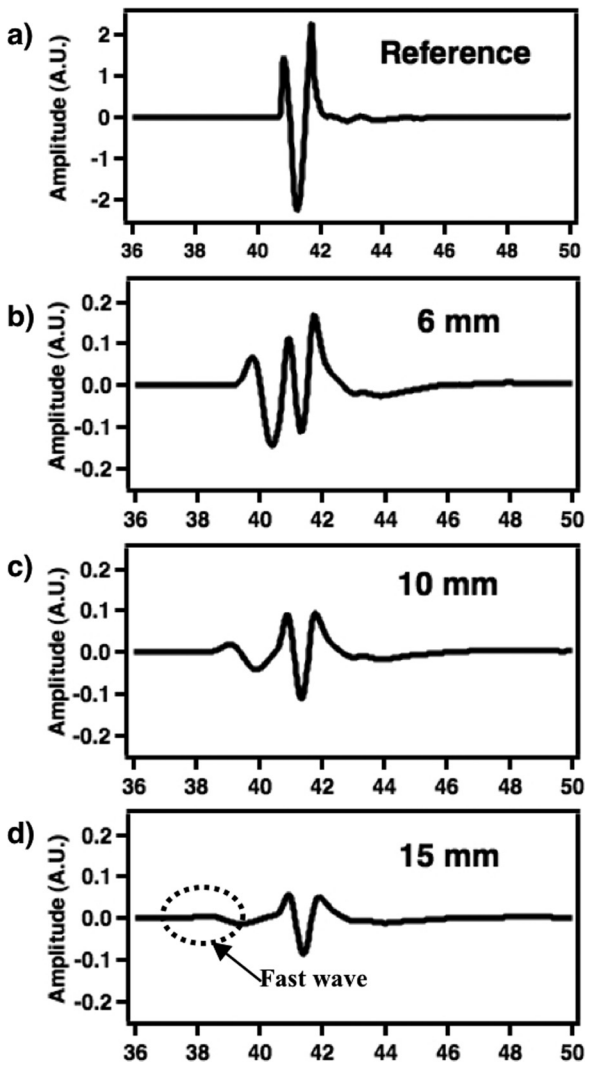


FIG. 1. (a) Reference (water-path only) waveform. Simulated sample waveforms traveling through (b) 6 mm, (c) 10 mm, and (d) 15 mm of sample.

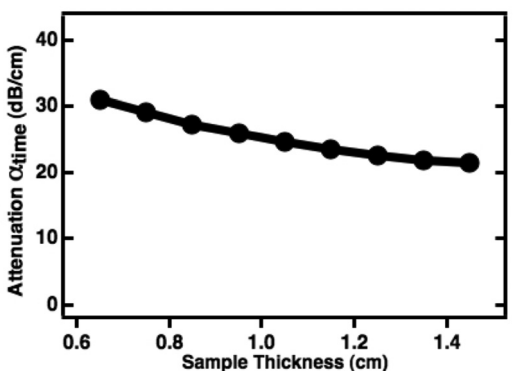


FIG. 2. The dependence of the attenuation, $\alpha_{\text{time}}$, of the fast wave on propagation distance using the time-domain analysis method.

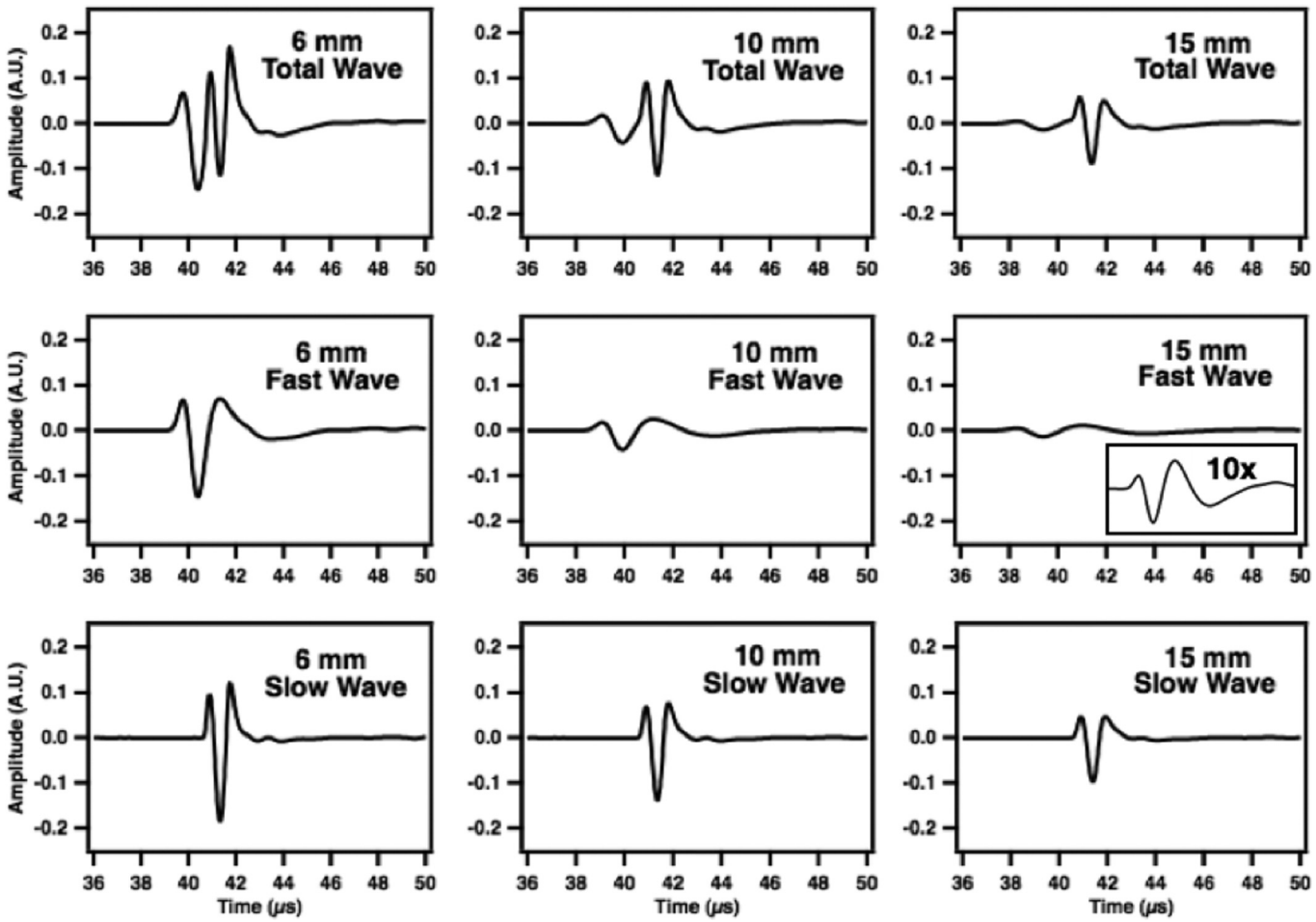


FIG. 3. The top panels show the sample waveform comprised of overlapping fast and slow waves for sample thicknesses of 6, 10, and 15 mm, respectively. The middle and bottom panels display the individual fast waves and individual slow waves, respectively, for the three sample thicknesses.

sample waveform into fast waves and slow waves. Representative examples of the individual fast waves and slow waves obtained from sample waveforms that have propagated through 6, 10, and 15 mm of sample are shown in Fig. 3. The fast waves, identified as those arriving earlier in time, have lower amplitudes than the slow waves.

For this method of analysis, the individual fast waves and slow waves were used in the log-spectral subtraction technique expressed in Eq. (7). Separating the fast and slow waves permits determination of the fast wave's attenuation coefficient without introducing interference artifacts from the slow wave. Similarly, the slow wave's attenuation coefficient can be calculated free from interference effects introduced by the fast wave. Performing the frequency domain analysis on the separated waveforms is essentially an inversion of the process used to simulate them from the values produced by the Bayesian parameter estimation. For this reason, it is guaranteed that this method will recover the attenuation coefficients used to initially simulate the waves. Furthermore, these attenuation coefficients cannot vary with distance. Figure 4 shows that, as required, the attenuation coefficient at 1 MHz of the fast wave, $\alpha_{\text{fast}}(f=1\ \text{MHz})$, and the attenuation coefficient at 1 MHz of the slow wave, $\alpha_{\text{slow}}(f=1\ \text{MHz})$, as a function of sample thickness display no dependence on the propagation distance, and that the numerical values of $\alpha_{\text{fast}}(f=1\ \text{MHz})$ and $\alpha_{\text{slow}}(f=1\ \text{MHz})$ are consistent with those used as input to the simulations. This result, though only a consistency check on the method, stands in contrast to the time-domain analysis shown above that seems to indicate a propagation distance dependence of the attenuation, despite the fact that the analyzed signals were simulated to have a strictly constant-with-propagation-distance attenuation coefficient.

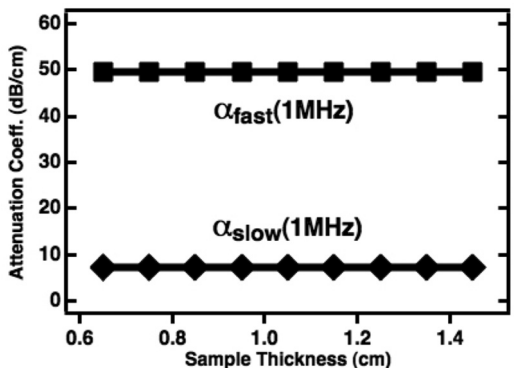


FIG. 4. The attenuation coefficient of the separated fast wave, $\alpha_{\text{fast}}(f)$, and slow wave, $\alpha_{\text{slow}}(f)$, at 1MHz as a function of propagation distance.

## IV. DISCUSSION

Cancellous bone can support the generation and propagation of two compressional wave modes, fast waves and slow waves. Depending on numerous factors, these two wave modes can overlap substantially and therefore interfere in the time-domain signal. Analysis of these overlapping waveforms can lead to unexpected conclusions. Conventional phase spectroscopy analysis performed on mixed mode signals as if only one wave were present can yield apparent negative dispersion.[14,15,17] Previous work has demonstrated, however, that when decomposed, the fast wave and slow wave each exhibit positive dispersion.[19,27] Negative dispersion has been measured not only in trabecular bone[29–33] and cortical bone[34] *in vitro* but also in trabecular bone-mimicking phantoms.[35,36] Several models have been proposed that predict negative dispersion including multilayer models,[31,37] multiple scattering models,[38] and independent scattering models.[39] The objective of this study was to investigate the potential value of separating the fast waves and slow waves for determining the attenuation properties of cancellous bone and to compare the results of time-domain and frequency-domain methods for the analysis of attenuation.

In this study, two methods of analysis were investigated using the same simulated cancellous bone data. The time-domain analysis method applied to the mixed-mode signal yielded a fast wave attenuation that started high at the beginning of propagation and then decreased as the wave traveled farther into the sample. However, the waves had been simulated with a strictly constant-with-propagation-distance attenuation coefficient. The frequency-domain analysis method applied to the separated fast waves and slow waves that made up that mixed-mode signal recovered the attenuation coefficients of both wave modes and did not introduce a dependence on the propagation distance. This finding demonstrates that application of time-domain based analysis to determine the attenuation properties of mixed mode waves can introduce an apparent dependence of the properties on propagation distance.

The ability to separate the fast and slow waves permits application of frequency-domain methods. If the separation is performed and the resulting waves are analyzed in the frequency domain, the known attenuation coefficients can be recovered. Figure 5 demonstrates that performing either these steps in isolation can introduce an apparent dependence on propagation distance. As illustrated, frequency-domain analysis of the unseparated wave [Fig. 5, panel (b)] and time-domain analysis of the separated waves [Fig. 5, panel (c)] both result in variable-with-distance apparent attenuation.

When the time-domain method was applied to the individual separated fast waves and slow waves, the attenuation of the fast wave, $\alpha_{\text{time}}^{\text{fast}}$, and the attenuation of the slow wave, $\alpha_{\text{time}}^{\text{slow}}$, both showed a dependence on sample thickness [Fig. 5, panel (c)]. This phenomenon results from estimating the attenuation from the time-domain amplitude of a broadband pulse. In the current system, a 1 MHz center-frequency, broadband pulse was used as the input signal. Typically, the

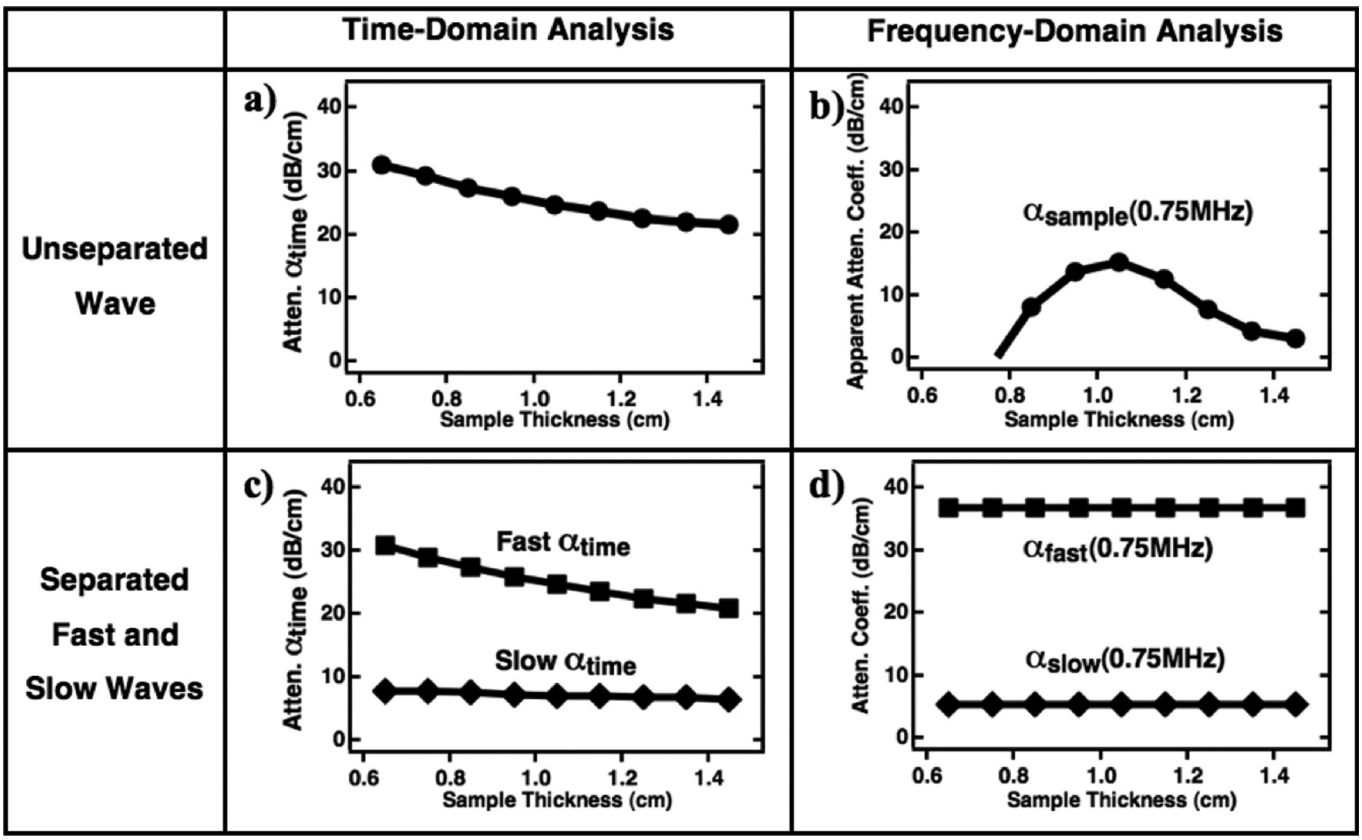


FIG. 5. The attenuation behavior as a function of sample thickness results when applying, panel (a): the time-domain method to the unseparated fast wave, panel (b): log-spectral subtraction to the entire sample wave, consisting of overlapping wave modes, panel (c): the time-domain method to the individual fast wave and slow wave, and panel (d): log-spectral subtraction to the separated fast wave and slow wave.

attenuation coefficient for both fast and slow waves increases with frequency in the range of interest. As a result, early in the propagation, the higher frequency components of the broadband signal are reduced more rapidly than the lower frequency signals, thus resulting in a signal exhibiting proportionally more of the lower frequency components. These lower frequency components are attenuated less with distance than the higher frequencies, resulting in a perceived attenuation coefficient that appears to decrease with distance. (Because of the shift to lower frequency components, to permit a better comparison with the time-domain analysis results, in Fig. 5 the frequency-domain attenuation coefficients for both the unseparated wave [panel (b)] and the separated fast and slow waves [panel (d)] are shown for $f = 0.75$ MHz rather than $f = 1$ MHz. In panel (b) the values of $\alpha_{\text{sample}}$ (0.75 MHz) are negative below sample thicknesses of 0.8 cm due to interference between the fast and slow waves.)

The frequency-domain analysis method does account for the broadband nature of the data; however, applying this method to the mixed-mode sample waveform still yields an apparent attenuation coefficient that depends on the thickness of the sample [Fig. 5, panel (b)]. This effect, observed previously in bone mimicking phantoms,[17,21] appears to be a result of interference between the fast and slow waves being perceived as attenuation. Figure 6 shows the apparent attenuation coefficient of the combined wave for three propagation distances, along with the known attenuation coefficients for the fast and slow wave. Panel (a) shows that when the signals have propagated a short distance, there is substantial interference between the two waves and a resulting anomalous attenuation coefficient. By the time the signals propagate to 10 mm [panel (b)] and 15 mm [panel (c)], the fast wave has been attenuated more than the slow wave, so the attenuation coefficient of the combined wave approaches the slow wave value. As illustrated in Fig. 4, the underlying attenuation coefficient of each mode can be obtained if separated fast waves and slow waves are available.

The results presented above might help in the interpretation of the recent study by Nagatani *et al.*[18] This previous work showed that the attenuation properties of cancellous bone could vary substantially on the scale of millimeters. The current work does not directly address this intrinsic inhomogeneity, but attempts to demonstrate that in a simulated sample with constant attenuation properties, some apparent variation can be introduced by the analysis methods. The nature and scale of the variation with depth reported by Nagatani *et al.* do not appear to be fully accounted for by effects originating from the analysis, but gaining a complete understanding of this complicated system will likely rely on isolating these effects.

As described previously, the complicated trabecular structure of cancellous bone represents a possible cause for the previously reported apparent decrease with distance of the attenuation coefficient.[18] The substantially higher speed of sound within the trabeculae (approximately 3500 m/s) relative to the lower speed of sound in the intervening marrow (approximately 1470 m/s)[40] causes the portions of the propagating signal that travel through the hard bone to advance much more quickly than the signal that propagates primarily through the interstitial marrow. When these faster signals have propagated only a short distance through the sample (relative to the pertinent scales determined by the trabecular spacing and by the wavelength of the sound), their phase fronts are generally misaligned. As a result, signals from a relatively large (compared to the wavelength) phase sensitive receiving aperture (real or simulated) will be subject to phase cancellation at its face.[41,42] This phase cancellation represents irretrievable loss of information that will appear as apparent attenuation. Similar examples of phase cancellation appearing as apparent attenuation in bone have been reported previously.[17,21,43]

If the fast wave is permitted to propagate farther into the sample, the phase front will tend toward realignment as the randomness induced by the trabeculae averages out over this longer path.[18] A phase sensitive receiver placed at the end of such a longer propagation path will be subject to less phase cancellation, and therefore less perceived attenuation. This phenomenon is described more fully in Nagatani *et al.* and is demonstrated in Fig. 10 of that paper.[18]

This phenomenon potentially complicates the interpretation of signals propagated through cancellous bone. However, because it is intrinsically linked to the size and spacing of trabeculae, this effect might ultimately be exploited to infer from apparent attenuation measurements the relevant length scales of the sample under investigation. Knowledge of these length scales might then be used to estimate clinically useful parameters such as the porosity and bone volume per total volume (BV/TV).

If the mixed-mode signal cannot be decomposed into its individual wave modes, then both the time-domain method and the frequency-domain method might introduce an apparent dependence on distance of the attenuation properties that

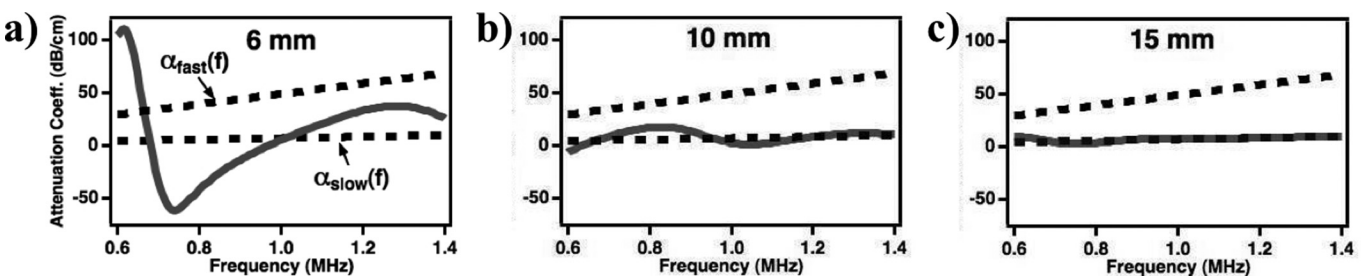


FIG. 6. The attenuation coefficients determined using the frequency-domain technique for the entire sample wave (solid line) and the separated fast and slow waves (dashed lines) for three propagation distances: 6 mm (panel a), 10 mm (panel b), and 15 mm (panel c).

is not representative of the underlying structure. Therefore, the ability to separate the fast waves and slow waves is of considerable importance. Bayesian probability theory is one method for determining the individual properties of the interfering wave modes,[19,27] but in principle any method that can isolate the two waves could be applied. Wear, for example, recently demonstrated that the modified least squares Prony's method was also able to decompose a mixed-mode signal and yield accurate estimates of its ultrasonic properties.[44,45]

The results of this study show that overlapping fast waves and slow waves can complicate the determination of the attenuation properties of cancellous bone. Specifically, the subtleties introduced by certain analysis methods applied to these temporally overlapped waves might represent, in part, an alternative explanation for the previously observed dependence on propagation distance of the attenuation properties of cancellous bone. Frequency domain analysis performed on the separated fast and slow waves was shown to be the least susceptible to such artifacts.

## ACKNOWLEDGMENT

This study was supported by NIH Grant R01-AR057433.

[1]D. Hans and M. A. Krieg, "The clinical use of quantitative ultrasound (QUS) in the detection and management of osteoporosis," IEEE Trans. Ultrason. Ferroelectr. Freq. Control **55**(7), 1529–1538 (2008).
[2]P. Laugier, "Instrumentation for in vivo ultrasonic characterization of bone strength," IEEE Trans. Ultrason. Ferroelectr. Freq. Control **55**(6), 1179–1196 (2008).
[3]M. L. Frost, G. M. Blake, and I. Fogelman, "Quantitative ultrasound and bone mineral density are equally strongly associated with risk factors for osteoporosis," J. Bone Miner. Res. **16**(2), 406–416 (2001).
[4]A. Hosokawa, "Effect of porosity distribution in the propagation direction on ultrasound waves through cancellous bone," IEEE Trans. Ultrason. Ferroelectr. Freq. Control **57**(6), 1320–1328 (2010).
[5]A. Hosokawa and T. Otani, "Acoustic anisotropy in bovine cancellous bone," J. Acoust. Soc. Am. **103**(5), 2718–2722 (1998).
[6]A. Hosokawa and T. Otani, "Ultrasonic wave propagation in bovine cancellous bone," J. Acoust. Soc. Am. **101**(1), 558–562 (1997).
[7]K. Mizuno, M. Matsukawa, T. Otani, P. Laugier, and F. Padilla, "Propagation of two longitudinal waves in human cancellous bone: An in vitro study," J. Acoust. Soc. Am. **125**(5), 3460–3466 (2009).
[8]G. Haiat, F. Padilla, F. Peyrin, and P. Laugier, "Fast wave ultrasonic propagation in trabecular bone: Numerical study of the influence of porosity and structural anisotropy," J. Acoust. Soc. Am. **123**(3), 1694–1705 (2008).
[9]L. Cardoso, F. Teboul, L. Sedel, C. Oddou, and A. Meunier, "In vitro acoustic waves propagation in human and bovine cancellous bone," J. Bone Miner. Res. **18**(10), 1803–1812 (2003).
[10]F. Padilla and P. Laugier, "Phase and group velocities of fast and slow compressional waves in trabecular bone," J. Acoust. Soc. Am. **108**, 1949–1952 (2000).
[11]K. Mizuno, M. Matsukawa, T. Otani, M. Takada, Mano Isao, and T. Tsujimoto, "Effects of structural anisotropy of cancellous bone on speed of ultrasonic fast waves in the bovine femur," IEEE Trans. Ultrason. Ferroelectr. Freq. Control **55**(7), 1480–1487 (2008).
[12]K. I. Lee, E. R. Hughes, V. F. Humphrey, T. G. Leighton, and M. J. Choi, "Empirical angle-dependent biot and mba models for acoustic anisotropy in cancellous bone," Phys. Med. Biol. **52**, 59–73 (2007).
[13]C. C. Anderson, A. Q. Bauer, K. R. Marutyan, M. R. Holland, M. Pakula, G. L. Bretthorst, P. Laugier, and J. G. Miller, "Phase velocity of cancellous bone: Negative dispersion arising from fast and slow waves, interference, diffraction, and phase cancellation at piezoelectric receiving elements," in *Bone Quantitative Ultrasound*, edited by P. Laugier and G. Haiat (Springer, Netherlands, 2011), pp. 319–330.
[14]K. R. Marutyan, M. R. Holland, and J. G. Miller, "Anomalous negative dispersion in bone can result from the interference of fast and slow waves," J. Acoust. Soc. Am. **120**(5), EL55–EL61 (2006).
[15]C. C. Anderson, K. R. Marutyan, M. R. Holland, K. A. Wear, and J. G. Miller, "Interference between wave modes may contribute to the apparent negative dispersion observed in cancellous bone," J. Acoust. Soc. Am. **124**(3), 1781–1789 (2008).
[16]K. R. Marutyan, M. R. Holland, and J. G. Miller, "Evidence that the negative dispersion in bone results from interference between fast and slow modes each with positive dispersion," Proc. IEEE Ultrason. Symp. **06CH37777C** 17–20 (2006).
[17]A. Q. Bauer, K. R. Marutyan, M. R. Holland, and J. G. Miller, "Negative dispersion in bone: The role of interference in measurements of the apparent phase velocity of two temporally overlapping signals," J. Acoust. Soc. Am. **123**(4), 2407–2414 (2008).
[18]Y. Nagatani, K. Mizuno, T. Saeki, M. Matsukawa, T. Sakaguchi, and H. Hosoi, "Numerical and experimental study on the wave attenuation in bone - FDTD simulation of ultrasound propagation in cancellous bone," Ultrasonics **48**, 607–612 (2008).
[19]C. C. Anderson, A. Q. Bauer, M. R. Holland, M. Pakula, P. Laugier, G. L Bretthorst, and J. G. Miller, "Inverse problems in cancellous bone: Estimation of the ultrasonic properties of fast and slow waves using Bayesian probability theory," J. Acoust. Soc. Am. **128**(5), 2940–2948 (2010).
[20]K. R. Waters and B. K. Hoffmeister, "Kramers-Kronig analysis of attenuation and dispersion in trabecular bone," J. Acoust. Soc. Am. **118**, 3912–3920 (2005).
[21]A. Q. Bauer, K. R. Marutyan, M. R. Holland, and J. G. Miller, "Is the Kramers-Kronig relationship between ultrasonic attenuation and dispersion maintained in the presence of apparent losses due to phase cancellation?," J. Acoust. Soc. Am. **122**, 222–228 (2007).
[22]M. O'Donnell, E. Jaynes, and J. G. Miller, "General relationships between ultrasonic attenuation and dispersion," J. Acoust. Soc. Am. **63**, 1935–1937 (1978).
[23]M. O'Donnell, E. Jaynes, and J. G. Miller, "Kramers-Kronig relationship between ultrasonic attenuation and phase velocity," J. Acoust. Soc. Am. **69**, 696–701 (1981).
[24]K. R. Waters, J. Mobley, and J. G. Miller, "Causality-imposed (Kramers-Kronig) relationships between attenuation and dispersion," IEEE Trans. Ultrason. Ferroelectr. Freq. Control **52**, 822–823 (2005).
[25]K. R. Waters, M. S. Hughes, J. Mobley, G. H. Brandenburger, and J. G. Miller, "On the applicability of Kramers-Kronig relations for ultrasonic attenuation obeying a frequency power law," J. Acoust. Soc. Am. **108**, 556–563 (2000).
[26]G. L Bretthorst, W. C. Hutton, J. R. Garbow, and J. J. H. Ackerman, "Exponential parameter estimation (in NMR) using Bayesian probability theory," Concepts Magn. Reson. **27A**, 55–63 (2005).
[27]K. R. Marutyan, G. L. Bretthorst, and J. G. Miller, "Bayesian estimation of the underlying bone properties from mixed fast and slow mode ultrasonic signals," J. Acoust. Soc. Am. **121**(1), EL8–EL15 (2007).
[28]S. L. Baldwin, K. R. Marutyan, M. Yang, K. D. Wallace, M. R. Holland, and J. G. Miller, "Measurements of the anisotropy of ultrasonic attenuation in freshly excised myocardium," J. Acoust. Soc. Am. **119**, 3130–3139 (2006).
[29]G. Haiat, F. Padilla, R. O. Cleveland, and P. Laugier, "Effects of frequency-dependent attenuation and velocity dispersion on in vitro ultrasound velocity measurements in intact human femur specimens," IEEE Trans. Ultrason. Ferroelectr. Freq. Control **53**, 39–51 (2006).
[30]R. Strelitzki and J. A. Evans, "On the measurement of the velocity of ultrasound in the os calcis using short pulses," Eur. J. Ultrasound **4**, 205–213 (1996).
[31]K. A. Wear, "A stratified model to predict dispersion in trabecular bone," IEEE Trans. Ultrason. Ferroelectr. Freq. Control **48**, 1079–1083 (2001).
[32]K. A. Wear, "Measurements of phase velocity and group velocity in human calcaneus," Ultrasound Med. Biol. **26**, 641–646 (2000).
[33]P. Droin, G. Berger, and P. Laugier, "Velocity dispersion of acoustic waves in cancellous bone," IEEE Trans. Ultrason. Ferroelectr. Freq. Control **45**(3), 581–592 (1998).
[34]G. Haiat, M. Sasso, S. Naili, and M. Matsukawa, "Ultrasonic velocity dispersion in bovine cortical bone: an experimental study," J. Acoust. Soc. Am. **124**(3), 1811–1821 (2008).
[35]K. I. Lee and M. J. Choi, "Phase velocity and normalized broadband ultrasonic attenuation in polyacetal cuboid bone-mimicking phantoms," J. Acoust. Soc. Am. **121**, EL263–EL269 (2007).
[36]K. A. Wear, "The dependencies of phase velocity and dispersion on trabecular thickness and spacing in trabecular bone-mimicking phantoms," J. Acoust. Soc. Am. **118**, 1186–1192 (2005).
[37]K. A. Wear, "Group velocity, phase velocity, and dispersion in human calcaneus in vivo," J. Acoust. Soc. Am. **121**(4), 2431–2437 (2007).

[38]G. Haiat, A. Lhemery, F. Renaud, F. Padilla, P. Laugier, and S. Naili, "Velocity dispersion in trabecular bone: Influence of multiple scattering and of absorption," J. Acoust. Soc. Am. **124**(6), 4047–4058 (2008).
[39]G. Haiat and S. Naili, "Independent scattering model and velocity dispersion in trabecular bone: comparison with a multiple scattering model," Biomech. Model. Mechanobiol. **10**, 95–108 (2011).
[40]P. Laugier, "The basic physics of ultrasound," in *Quantitative Ultrasound: Assessment of Osteoporosis And Bone Status*, edited by C. F. Njeh, D. Hans, T. Fuerst, C.C. Gluer and H.K. Genant (Martin Dunitz Ltd., London, 1999), p. 56.
[41]L. J. Busse and J. G. Miller, "Response characteristics of a finite aperture, phase insensitive ultrasonic receiver based upon the acoustoelectric effect," J. Acoust. Soc. Am. **70**(5), 1370–1376 (1981).
[42]L. J. Busse and J. G. Miller, "Detection of spatially nonuniform ultrasonic radiation with phase sensitive (piezoelectric) and phase insensitive (acoustoelectric) receivers," J. Acoust. Soc. Am. **70**(5), 1377–1386 (1981).
[43]K. A. Wear, "The effect of phase cancellation on estimates of calcaneal broadband ultrasound attenuation in vivo," IEEE Trans. Ultrason. Ferroelectr. Freq. Control **54**(7), 1352–1359 (2007).
[44]K. A. Wear, "Decomposition of two-component ultrasound pulses in cancellous bone using modified least squares Prony method-Phantom experiment and simulation," Ultrasound Med. Biol. **36**(2), 276–287 (2010).
[45]K. A. Wear, "Cancellous bone analysis with modified least squares Prony's method and chirp filter: Phantom experiments and simulation," J. Acoust. Soc. Am. **128**(4), 2191–2203 (2010).